Published in final edited form as:
*Cancer Cell*. 2014 May 12; 25(5): 652–665. doi:10.1016/j.ccr.2014.03.016.

# MLL3 Is a Haploinsufficient 7q Tumor Suppressor in Acute Myeloid Leukemia

**Chong Chen**[1], **Yu Liu**[1], **Amy R. Rappaport**[2], **Thomas Kitzing**[1], **Nikolaus Schultz**[3], **Zhen Zhao**[1], **Aditya S. Shroff**[1], **Ross A. Dickins**[4], **Christopher R. Vakoc**[2], **James E. Bradner**[5], **Wendy Stock**[6], **Michelle M. LeBeau**[6], **Kevin M. Shannon**[7], **Scott Kogan**[8], **Johannes Zuber**[2,9], and **Scott W. Lowe**[1,10,*]

[1]Cancer Biology and Genetics Program, Memorial-Sloan Kettering Cancer Center, New York, NY 10065, USA

[2]Cold Spring Harbor Laboratory, One Bungtown Road, Cold Spring Harbor, NY 11724, USA

[3]Computational Biology Center, Memorial-Sloan Kettering Cancer Center, New York, NY 10065, USA

[4]Molecular Medicine Division, Walter and Eliza Hall Institute of Medical Research, Parkville, VIC 3052, Australia

[5]Department of Medical Oncology, Dana-Farber Cancer Institute, Harvard Medical School, 44 Binney Street, Boston, MA 02215, USA

[6]Section of Hematology/Oncology, University of Chicago, Chicago, IL 60637, USA

[7]Department of Pediatrics, School of Medicine, University of California, San Francisco, San Francisco, CA 94143, USA

[8]Department of Laboratory Medicine & Helen Diller Family Comprehensive Cancer Center, University of California, San Francisco, San Francisco, CA 94158, USA

[9]Research Institute of Molecular Pathology, 1030 Vienna, Austria

[10]Howard Hughes Medical Institute, Memorial-Sloan Kettering Cancer Center, New York, NY 10065, USA

## SUMMARY

Recurring deletions of chromosome 7 and 7q [−7/del(7q)] occur in myelodysplastic syndromes and acute myeloid leukemia (AML) and are associated with poor prognosis. However, the identity of functionally relevant tumor suppressors on 7q remains unclear. Using RNAi and CRISPR/Cas9 approaches, we show that an ~50% reduction in gene dosage of the mixed lineage leukemia 3



*Correspondence: lowes@mskcc.org.

**SUPPLEMENTAL INFORMATION**

Supplemental Information includes Supplemental Experimental Procedures, six figures, and one table and can be found with this article online at http://dx.doi.org/10.1016/j.ccr.2014.03.016.

**ACCESSION NUMBERS**

The GEO accession number for the Illumina gene expression profiling data reported in this paper is GSE54313.

(*MLL3*) gene, located on 7q36.1, cooperates with other events occurring in −7/del(7q) AMLs to promote leukemogenesis. Mll3 suppression impairs the differentiation of HSPC. Interestingly, Mll3-suppressed leukemias, like human −7/del(7q) AMLs, are refractory to conventional chemotherapy but sensitive to the BET inhibitor JQ1. Thus, our mouse model functionally validates MLL3 as a haploinsufficient 7q tumor suppressor and suggests a therapeutic option for this aggressive disease.

## INTRODUCTION

Acute myeloid leukemia (AML) comprises a series of clinically and genetically heterogeneous cancers that are caused by mutations that drive aberrant proliferation and impaired differentiation of hematopoietic stem and progenitor cells (HSPC). Over the past several years, genomic studies have identified a number of genes that are affected by recurrent somatic point mutations in different AML subtypes, information that in turn has led to a greater understanding of AML biology and suggested new treatments for these diseases (Patel et al., 2012). However, some subsets of AML harbor large chromosomal deletions the impact of which on leukemia biology and treatment is poorly understood. For example, monosomy 7 or large deletions of 7q (−7/del(7q)) are associated with myelodysplastic syndrome (MDS) and AML, and often occur together with −5/del(5q) and del(17p) in the context of complex karyotype (CK) AML (Mrózek, 2008). Such mutations are also common in myeloid neoplasms arising in patients treated with alkylating agents for a previous cancer (Qian et al., 2010). Unlike AMLs with other abnormalities, these malignancies are largely refractory to conventional chemotherapy and thus represent an AML subset for which new treatments are urgently needed (Döhner et al., 2010; Grimwade et al., 2010).

Candidate tumor suppressor genes have been identified in some deletions found in AML, such as those arising on chromosome 17p that often target the *TP53* tumor suppressor, and on chromosome 5q (e.g., *EGR1*; Joslin et al., 2007 and *CTNNA1*; Liu et al., 2007). However, less is known about the nature of potential AML tumor suppressors on 7q. Indeed, the 7q deletions occurring in AML are often quite large, with minimally deleted regions identified at 7q21.3 (Asou et al., 2009), 7q22 (Le Beau et al., 1996), and 7q34-36 (Itzhar et al., 2011; Rücker et al., 2006). Intensive efforts to uncover “second hit” mutations on the nondeleted allele have been largely unsuccessful and no 7q gene has been functionally validated as a tumor suppressor in the context of AML.

One candidate 7q tumor suppressor is the mixed lineage leukemia *3* (*MLL3*) gene, located on 7q36.1. MLL3 is a member of the MLL protein family and contains a SET domain capable of methylating lysine 4 on histone H3 (H3K4), a histone mark associated with active transcription (Shilatifard, 2012). Also, by virtue of its association with other proteins, such as the histone H3 demethylase UTX, complexes containing MLL3 can trigger demethylation of histone H3 K27, which when methylated is linked to transcriptional repression (Herz et al., 2012; Lee et al., 2007; Tie et al., 2012). *MLL3* is related to *MLL1*, which is involved in multiple recurring translocations in acute lymphoid leukemia (ALL) and AML. Somatic mutations in *MLL3* are one of the most frequent events in human cancer, with missense

mutations occurring throughout its open reading frame present in a wide range of tumor types (Gui et al., 2011; Ong et al., 2012; Parsons et al., 2011; Zang et al., 2012). Nonetheless, *MLL3* is an extremely large gene (1,700 kb; and MLL3 protein is 530 KDa), leading to speculation as to whether its high mutation rate might simply reflect the increased probability of sustaining passenger events (Jones et al., 2008).

Consistent with a role for MLL3 in suppressing tumorigenesis, mice subjected to transposon mutagenesis often develop tumors harboring common insertion sites at the *Mll3* locus (Mann et al., 2012; March et al., 2011), and those harboring targeted deletions of the Mll3 SET domain are prone to ureter epithelial tumors that are exacerbated in a $p53^{+/-}$ background (Lee et al., 2009). Nevertheless, Mll3 mutant mice do not develop leukemia. In this study, we investigated the in vivo function of Mll3 in hematopoiesis and leukemogenesis. Furthermore, we studied the drug response and the susceptibility of Mll3 deficient AML.

## RESULTS

### Analysis of 7q Alterations in Human Myeloid Neoplasms

As a step toward understanding and modeling the genetic and molecular changes that contribute to the aggressive nature of complex karyotype (CK) AML, we analyzed the genome pro-files of adult AML harboring normal and complex karyotypes. By analyzing array-based comparative genomic hybridization data sets produced in our laboratory, we identified one relapse normal karyotype (NK) AML case harboring a focal deletion (8.8 Mb) at 7q35-36 encompassing the *MLL3* gene (Figure S1A available online). This deletion was not present at diagnosis, suggesting its acquisition was associated with therapy resistance. We also identified a CK AML with a 7q deletion and a 17q deletion encompassing the neurofibromatosis 1 gene (*NF1*), and two additional del(7q) cases with highly focal *NF1* deletions (Figure 1A). NF1 is a RAS-GAP that when heterozygously mutated predisposes patients to develop juvenile myelomonocytic leukemia that progresses to AML upon mutation of the second allele (Balgobind et al., 2008); its inactivation promotes myeloproliferative disease in mice (Le et al., 2004).

Interestingly, *MLL3* is one of the most frequently mutated genes in human cancer (Kandoth et al., 2013; Lawrence et al., 2014) and analysis of chromosome copy number alterations of more than 8,000 human cancers identified a single deleted peak in 7q35-36, which perfectly matches the *MLL3* locus (Figure S1B). Moreover, in analyzing a larger set of 200 AML cases produced by the Cancer Genome Atlas consortium (Cancer Genome Atlas Research Network, 2013), we identified 12 samples with chromosome 7 loss (−7), 12 samples with 7q deletions (del(7q)) including *MLL3*, and one case with a nonsense mutation in *MLL3* (Figure 1B and Figure S1C). By integrating SNP and somatic mutation data for this panel of AML samples, we noticed that Ras pathway mutations (*NF1* deletions or activating mutations in *NRAS, KRAS*, or *PTPN11*) occurred in ten of the 24 −7/del(7q) cases, which is significantly higher than that in cases with chromosome 7 intact (chi square test, $p = 0.011$). The single case with a *MLL3* nonsense mutation also contained an $NRAS^{G12D}$ mutation (Figure 1C). Consistent with a previous report (Rücker et al., 2012), alterations in *TP53* were detected in ten of 24 −7/del(7q) AMLs, a significantly higher frequency than the

samples with intact chromosome 7 (chi square test, $p < 0.0001$; Figure 1C). Interestingly, all three −7/del(7q) patients with *NF1* deletions also had *TP53* deletions that were often but not always associated with losses on 5q. Therefore, −7/del(7q) is associated with Ras pathway mutations and *TP53* alterations in AML. Based on these data, we reasoned that MLL3 loss might cooperate with hyperactive RAS signaling and *p53* inactivation in myeloid leukemogenesis.

## Mll3 Suppression Cooperates with Other Lesions to Drive Leukemogenesis

To study the effect of Mll3 suppression during leukemogenesis, we used a transplantation-based mouse modeling approach that has been used to characterize driving genetic events in AML and other hematologic malignancies (Zhao et al., 2010; Zuber et al., 2009). In this approach, various genetic elements are introduced into HSPC by retroviral mediated gene transfer, and "mosaic" animals are produced following transplantation of these modified cells into syngeneic recipient mice. Shorthairpin RNAs (shRNAs) can be transduced to suppress gene function by RNA interference (Dickins et al., 2005; Silva et al., 2005), which can model the impact of both classic "two-hit" and haploinsufficient tumor suppressors (Figure 2A). By introducing shRNAs targeting *Mll3* and/or *Nf1* into *p53* null HSPC and studying their tumorigenic potential, we can eliminate the requirement for intercrossing up to six mutant alleles. As a first step toward examining the impact of Mll3 and Nf1 suppression on leukemia, we produced multiple shRNAs capable of efficiently suppressing Mll3 or Nf1 protein (Figure S2A). Of note, the *Mll3* shRNAs had no homology to any other gene (data not shown) and did not affect expression of Mll4, its most closely related gene (Figure S2B). shRNAs targeting *Mll3* were linked to mCherry and those targeting *Nf1* were linked to GFP, allowing cells transduced with each shRNA to be tracked independently in vivo. Because *TP53* mutations frequently occur together with −7/del(7q) alterations in the context of CK AML (Figure 1; Rücker et al., 2012), we used HSPC from E14.5 *p53* null mice as the target cell populations. The recipient animals were monitored for evidence of hematologic disease and overall survival.

We observed a striking interaction between suppression of Nf1 and Mll3 on leukemogenesis. Consistent with results from *p53* null mice (Donehower et al., 1992), mice transplanted with $p53^{-/-}$ HSPC transduced with a control vector eventually succumbed to a hematologic malignancy with a median survival of 125 days (Figure 2B). Whereas suppression of Nf1 alone produced a modest acceleration of disease (median survival = 103 days, $p = 0.01$ versus sh*Ren*), Mll3 suppression had no effect on survival compared to mice transduced with neutral shRNA (sh*Mll3-1*: median survival = 125 days, $p = 0.79$ versus sh*Ren*; sh*Mll3-2*: median survival = 121.5 days, $p = 0.17$ versus sh*Ren*). In contrast, co-suppression of Nf1 and Mll3 using two independent shRNAs induced a dramatic reduction in survival, leading to death of the mice within 2 months after transplantation (sh*Mll3*-1;sh*Nf1*: median survival = 61.5 days, $p < 0.0001$ versus sh*Ren*; and sh*Mll3*-2;sh*Nf1*: median survival = 57.5 days, $p < 0.0001$ versus sh*Ren*). A significant increase in peripheral white blood cell (WBC) counts and anemia was noted in recipients of sh*Mll3*;sh*Nf1;*$p53^{-/-}$ cells (hereafter referred to as MNP) shortly before sacrifice, indicative of leukemic outgrowth with suppression of normal hematopoiesis (Figures 2C, 2D, and S2C). Interestingly, only malignancies arising in mice receiving HSPC transduced with both

*Mll3* and *Nf1* shRNAs showed a predominantly mCherry/GFP double-positive population (Figures 2E and S2D), confirming that cosuppression of Mll3 and Nf1 provided a strong selective advantage during disease expansion. Of note, co-expression of *Nf1* and *Mll3* shRNAs was not oncogenic in wild-type HSPC, because mice transplanted with these cells showed no evidence of leukemia for up to 6 months (data not shown). Thus, the dramatic onset of disease by *Mll3* shRNAs required suppression of Nf1 and inactivation of p53.

## Mll3 Suppression Promotes the Development of Myeloid Leukemia

Pathological analyses and immunophenotyping revealed that mice transplanted with $p53^{-/-}$ HSPC transduced with control shRNAs typically displayed an enlarged thymus consisting primarily of $CD3^+$ T cells (Figures S3A–S3D), indicative of the thymic lymphoma that has been described in germline $p53^{-/-}$ mice (Donehower et al., 1992; Jacks et al., 1994). Whereas mice transplanted with sh*Nf1*-expressing HSPC developed myeloid disease in some experiments (data not shown), the majority of mice developed thymic lymphomas similar to those described above (Figures 3A, 3B, and S3D). Consistent with the observation that cells transduced with sh*Mll3* alone did not accelerate disease onset or contribute to the malignant population recovered at death (Figure 2), mice transplanted with sh*Mll3;*$p53^{-/-}$ HSPC presented identically to those transplanted with $p53^{-/-}$ HPSCs (Figures S3A–S3D).

In stark contrast, moribund recipients of HPSCs expressing both sh*Mll3* and sh*Nf1* displayed hepatomegaly and massive splenomegaly (Figures S3B and S3C), resulting from extramedullary hematopoiesis and the infiltration of malignant cells (Figure 3A). Bone marrow and spleens of 19/20 transplanted mice were filled with leukemic cells that expressed myeloid lineage markers ($CD3^-$;$B220^-$;c-$kit^+$;Mac-$1^+$; Figure 3B). Accordingly, peripheral smears revealed leukocytosis with increased numbers of neutrophils, monocytes, and blasts (Figure 3A). These phenotypes were not observed in any of the single knockdown or negative controls. Of note, neoplastic cells co-expressing sh*Mll3* and sh*Nf1* produced AML and rapid death in transplanted secondary recipients, indicating that they were fully transformed (Figures 3C and 3D). Thus, Mll3 and Nf1 suppression switches the lineage of hematologic cancers harboring *p53* deletions from T cell lymphoma to AML.

## Mll3 Is a Haploinsufficient Tumor Suppressor in AML

Mutations and deletions of *MLL3* on 7q have been only noted on one allele, suggesting that MLL3 is a haploinsufficient tumor suppressor (Jerez et al., 2012). To test this, we measured the Mll3 expression level in sh*Mll3*-induced AML. Interestingly, although acute expression of *Mll3* and *Nf1* shRNAs in mouse embryonic fibroblasts (MEFs) produces substantially greater Mll3 and Nf1 suppression, respectively (Figure S2A), the Mll3 levels present in MNP AML were ~50% of control untransformed 32D cells or *MLL-AF9;*$Nras^{G12D}$ (MAR) AML cells (Figures S4A and S4B). Similarly, we also observed approximate 50% Nf1 repression by shNf1 in MNP AML compared to MAR AML (Figure S4C). Because the initial transduced populations are polyclonal, likely with a range of Mll3 knockdown, our data imply that clones with intermediate Mll3 knockdown have a preferential advantage during leukemogenesis. The haploinsufficiency of Mll3 in MNP AML mimics that in human −7/del(7q) hematopoietic malignancy (Figure S4D).

To further support our hypothesis that *Mll3* is a haploinsufficient tumor suppressor in AML, we applied in vivo CRISPR/Cas9 genome editing technology (Cong et al., 2013; Mali et al., 2013) to disrupt *Mll3* (Figure 4A). Consistent with Mll3 knockdown by shRNAs, CRISPR/Cas9 targeting *Mll3* (cr_*Mll3*) accelerated disease compared to a control CRISPR/Cas9 (cr_*Ctrl*) targeting a noncoding region on mouse chromosome 8 (Figure 4B). Recipient mice transplanted with cr_*Mll3*;sh*Nf1;p53*$^{-/-}$ HSPC also had dramatically higher WBC counts than cr_*Ctrl*;sh*Nf1;p53*$^{-/-}$ recipients at their respective time of sacrifice (Figure 4B). As was observed using shRNAs, pathological studies and flow cytometry indicated that recipients of cr_*Mll3*;sh*Nf1;p53*$^{-/-}$ HSPC developed AML whereas mice receiving cr_*Ctrl*;sh*Nf1;p53*$^{-/-}$ HSPC developed T-ALL (Figures 4C and 4D). All of the leukemic cells in recipient mice transplanted with cr_*Mll3*;sh*Nf1;p53*$^{-/-}$ HSPC expressed sh*Nf1*, indicating that *Nf1* suppression is required for tumorigenesis in this setting.

CRISPR-Cas9-directed mutagenesis can produce mutations in one or both alleles of the target gene, which can be revealed by sequencing of genomic DNA around the target site (Cong et al., 2013; Mali et al., 2013). Indeed, on-target inactivating *Mll3* mutations were detected in cr_*Mll3*;sh*Nf1;p53*$^{-/-}$ AML (Figure 4E). Remarkably, sequencing of individual cr_*Mll3*;sh*Nf1;p53*$^{-/-}$ AML clones revealed both wild-type and mutant alleles in five of six samples analyzed; whereas on-target mutation was not detected in the last clone. Consequently, these leukemia cells were heterozygous for intact Mll3, again suggesting that leukemogenesis selects for partial but not complete Mll3 inactivation. These data, together with results using RNAi, are consistent with the genomic analyses of human leukemia and provide compelling evidence that Mll3 is a haploinsufficient tumor suppressor in AML.

### Mll3 Suppression Impairs Differentiation and Produces an MDS-like State

Mutations in AML are generally considered to contribute to leukemogenesis by promoting proliferation and/or survival or impairing myeloid differentiation together leading to the formation of leukemic blasts (Kelly and Gilliland, 2002). Because Nf1 loss triggers the aberrant proliferation of hematopoietic cells (Bollag et al., 1996), we tested whether Mll3 suppression might impair the differentiation of HSPC in vitro and in vivo. Accordingly, relative to sh*Ren;p53*$^{-/-}$ controls, in vitro cultured sh*Mll3;p53*$^{-/-}$ HSPC displayed increased proliferation (as assessed by bromodeoxyuridine incorporation) and frequency of c-kit$^{+}$ cells (Figures S5A and S5B). Then we performed a competitive reconstitution assay and analyzed hematopoietic cell populations in recipient mice at 6 weeks after transplantation by immunophenotyping (Zuber et al., 2011; Figure 5A). Mll3 suppression significantly increased the frequency and absolute number of long-term hematopoietic stem cells (LT-HSC; Flt3$^{-}$lin$^{-}$Sca-1$^{+}$c-kit$^{+}$CD150$^{+}$ CD48$^{-}$CD34$^{-}$), while decreasing short-term HSC (ST-HSC; Flt3$^{-}$lin$^{-}$Sca-1$^{+}$c-kit$^{+}$CD150$^{+}$CD48$^{+}$CD34$^{-}$) and multipotent progenitors (MPP; Flt3$^{-}$lin$^{-}$Sca-1$^{+}$c-kit$^{+}$CD150$^{-}$CD48$^{+}$ CD34$^{-}$), indicating the differentiation of LT-HSC to ST-HSC and MPP was impaired (Figures 5B, 5C, and S5C). Accordingly, sh*Mll3;p53*$^{-/-}$ mice had fewer common myeloid progenitors (Flt3$^{-}$lin$^{-}$Sca-1$^{-}$c-kit$^{+}$CD34$^{+}$CD16/32$^{-}$) and granulocyte/monocyte progenitors (Flt3$^{-}$lin$^{-}$Sca-1$^{-}$c-kit$^{+}$CD34$^{+}$CD16/32$^{+}$) than controls (Figures 5D, S5C, and S5D). These changes were associated with significant bone marrow (BM) hypocellularity in sh*Mll3;p53*$^{-/-}$ recipients, although at this time posttransplantation, the frequency of sh*Mll3*-expressing BM cells was increased (Figure 5E). Taken together,

these results indicate that Mll3 is required for efficient differentiation of HSPC from LT-HSC to ST-HSC, MPP, and more committed myeloid progenitors.

Differentiation defects of HSPC can trigger MDS, a stem cell disease characterized by ineffective hematopoiesis and dysplasia that is frequently associated with −7/del(7q) alterations (Corey et al., 2007). In mice, MDS is characterized by cytopenia in one or multiple lineages in peripheral blood, defects in myeloid cell maturation in association with dysplastic myeloid lineage cells and/or blasts, and the absence of fully transformed leukemia (Kogan et al., 2002). To determine whether Mll3 suppression produces additional MDS phenotypes, we further characterized the distribution, morphology, and functionality of hematopoietic cells obtained from mice reconstituted with sh*Mll3;p53*$^{-/-}$ HSPC in comparison to sh*Ren;p53*$^{-/-}$ controls. sh*Mll3;p53*$^{-/-}$ recipients displayed a decreased WBC count, largely owing to a marked reduction in myeloid lineage cells and platelets (Figures 5F and S5E). Importantly, these defects were not due to decreased fitness or apoptosis of these cells (Figure 5G), indicating a maturation defect. Significant dysplasia was observed in multiple lineages in peripheral blood and BM of sh*Mll3;p53*$^{-/-}$ recipients but not controls (Figure 5H). Finally, sh*Mll3;p53*$^{-/-}$ BM cells had reduced colony formation capacity (Figure 5I), which is in agreement with the reduction in committed progenitors noted above (Figure 5D). Whereas the above observations meet the criteria of MDS in mice, sh*Mll3*-expressing HSPC were eventually depleted 2 months after transplantation (Figures 2E, S5F, and S5G), suggesting that additional events on 7q may be required to sustain this MDS-like state. Nonetheless, our studies clearly show that Mll3 suppression impairs differentiation of myeloid lineage in mice and is associated with phenotypes linked to −7/del(7q) in humans.

## Mll3 Suppression Produces a Transcriptional Profile Linked to Human MDS

As a first step toward understanding the molecular mechanism whereby Mll3 suppression impairs differentiation and contributes to AML, we compared the transcriptional profiles of fluorescence-activated cell sorted (FACS) sh*Mll3;p53*$^{-/-}$ and sh*Ren;p53*$^{-/-}$ HSPC using Illumina microarray analysis (Table S1). Differentially expressed genes were those in which expression was altered by more than 1.5-fold with $p < 0.05$ (Figure 6A). Consistent with the predicted impact of H3K4 methylation via MLL3 complexes on stimulating transcription (Shilatifard, 2012), sh*Mll3;p53*$^{-/-}$ HSPC displayed a preponderance of underexpressed genes (44 downregulated versus 11 upregulated). There was high concordance between the signatures of the two *Mll3* shRNAs, which further argues against an off-target effect of the two *Mll3* shRNAs (Figure 6B). Of these, genes showing the greatest fold-change upon Mll3 suppression were validated by quantitative RT-PCR (qRT-PCR) using RNA isolated from FACS purified LT-HSCs (Figure 6C), thus minimizing the possibility that altered gene expression was solely due to changes in cell composition between control and sh*Mll3* recipients. Consistent with the functional studies above (Figure 5), gene ontology analysis revealed that genes downregulated in response to Mll3 inhibition were enriched in functional categories linked to hematopoietic differentiation, including “antigen processing and presentation” ($p = 0.001$), “immune response” ($p = 0.003$), and multiple lineage differentiation (T cell differentiation, $p = 0.011$, myeloid cell differentiation, $p = 0.018$ and leukocyte differentiation, $p = 0.037$; Figure 6D).

Gene set enrichment analysis (GSEA) was used to determine whether the transcriptional signature produced by Mll3 suppression was significantly related to other previously studied conditions (Subramanian et al., 2005). The global expression changes produced in sh*Mll3;p53*$^{-/-}$ HSPC (compared to sh*Ren;p53*$^{-/-}$ HSPC) positively correlated with a hematopoietic early progenitor-associated gene signature (Ivanova et al., 2002; normalized enrichment score [NES] = 1.89 and false discovery rate [FDR] q = 0.0) but was negatively correlated with the gene signature of mature hematopoietic cells (NES = −2.22, FDR q = 0.0; Figure 6E and Table S1). Additionally, genes differentially expressed in sh*Mll3;p53*$^{-/-}$ HSPC were also enriched for genes previously identified as part of a leukemia stem cell signature (Somervaille et al., 2009; LSC_UP: NES = 1.48, FDR q = 0.02; LSC_DN: NES = −2.20, FDR q = 0.0; Figure 6F and Table S1). Strikingly, there was a significant correlation between genes down-regulated by *Mll3* shRNAs in murine HSPC and a signature of genes downregulated in HSCs derived from patients with MDS compared to normal HSCs (Pellagatti et al., 2010; NES = −2.17, FDR q = 0.0). Furthermore, the downregulated signature of −7/7q MDS HSC versus normal karyotype MDS was also negatively enriched in sh*Mll3;p53*$^{-/-}$ HSPC (NES = −2.14, FDR q = 0.0; Figure 6G and Table S1). Hence, Mll3 suppression is associated with impaired differentiation and produces a gene signature used to define −7/del(7q) MDS. The latter observation further implies that Mll3 repression is a major driver of phenotypes produced by −7/del(7q) alterations in patients.

Mll3 promotes transcriptional activation by methylating histone H3 at lysine 4; additionally, Mll3 exists in a larger complex that contains components capable of demethylating histone H3 at K27, further promoting transcriptional activation by removing this repressive mark (Lee et al., 2007; Shilatifard, 2012; Tie et al., 2012). To test whether Mll3 regulates its target genes by affecting gene-specific histone modifications, we performed a series of chromatin immunoprecipitation (ChIP) assays using antibodies against H3K4me3 and H3K27me3. qPCR following ChIP using gene-specific primers showed that there was significantly reduced H3K4me3 and increased H3K27me3 at the loci of all downregulated genes tested (Figure 6H). Although consistent with a direct effect of Mll3-containing complexes (Herz et al., 2012; Shilatifard, 2012), it remains to be determined whether Mll3 and the compass-like complex directly modify the histone markers of these target genes. Regardless, our data indicate that Mll3 suppression produces a repressive chromatin context on genes linked to differentiation, an effect that likely contributes to differentiation defects in MDS and AML.

## Mll3 Suppressed Leukemia Is Resistant to Conventional Chemotherapy but Responds to BET Inhibition

Patients with −7/del(7q) AML have a dismal prognosis, in large part because such leukemias respond poorly to chemotherapy and quick relapse (Haferlach, 2008; Rücker et al., 2012). To test this in our model, we used a regimen of cytarabine (araC) and doxorubicin (Doxo) therapy that approximates the standard induction chemotherapy used to treat patients with AML (Zuber et al., 2009). Consistent with previous reports, mice harboring *AML1-ETO;Nras*$^{G12D}$ AMLs responded well to therapy, whereas mice harboring MAR leukemia were relatively resistant and obtained only a modest survival advantage (Figure 7A). Mice harboring MNP AMLs displayed the worst prognosis, showing little to no clearance of leukemic blasts from the BM and no survival benefit (Figures 7A and 7B). Similarly, MNP

AML cells were also more resistant to treatment with either AraC or Doxo than MAR AML cells in vitro (Figures S6A and S6B). In a more direct experiment, Mll3 suppression in otherwise chemosensitive AML1-ETO-induced AML cells also produced chemoresistance in vitro and in vivo (Figures 7C, 7D, S6C, and S6D). These data imply that Mll3 suppression, alone or in the context of other CK AML lesions, can promote therapy resistance.

Currently, there are no animal models of CK AML for use in preclinical studies to test new agents that might be effective in treating these patients. Given the similarly poor response of MNP AML and human CK AML to conventional therapy, we tested whether our system might be used to generate preclinical support for more effective agents. Recently, our group and others identified the bromodomain and extra-terminal (BET) family protein Brd4 as a therapeutic target in AML and inhibition of Brd4 abolished the abnormal self-renewal reprogram in leukemia stem cells through a Myc-dependent mechanism (Dawson et al., 2011; Zuber et al., 2011). Because Mll3 suppression affected a leukemia stem cell signature that was subsequently linked to Myc activity (Figure 6E), we tested whether murine and human leukemia cells harboring this alteration would be likewise sensitive to BET inhibition.

Despite their profound resistance to chemotherapy (Figures 7A, 7B, S6A, and S6B), MNP AML cells were highly sensitive to the BET inhibitor JQ1, which induced marked differentiation and apoptosis (Figures 7E and S6E–S6G). Similarly, JQ1 treatment of mice bearing MNP leukemia caused clearance of leukemic cells from the peripheral blood without substantial effects on red blood cell and platelet counts, thereby doubling the lifespan of leukemic mice (Figures 7F, 7G, and S7H). Human AML cells with −7/del(7q) (UoCM1 and Mono7) were also sensitive to JQ1 treatment in a manner similar to cell lines harboring genetic alterations associated with better prognoses (Figure 7H). As has been reported for other leukemia genotypes, JQ1 treatment of both murine MNP AML and 7q altered human AML lines produced a rapid decrease in Myc protein and mRNA expression, with consequent reduction of Myc transcriptional targets (Figures S7I–S7K), and enforced Myc expression attenuated the antiproliferative response to JQ1 (Figure S7L). Thus, although −7/del(7p) AML harboring Mll3 suppression are chemoresistant, they remain sensitive to BET inhibition. These data support the preclinical utility of our model and suggest a possible therapeutic approach for the treatment of patients with −7/del(7q) AML.

## DISCUSSION

Our studies identify *MLL3* as a tumor suppressor gene on 7q, the attenuation of which contributes to the aggressive nature of certain forms of AML. Although *MLL3* is one of the most frequently mutated and deleted genes in human cancer, the biological significance of these mutations are not known (Kandoth et al., 2013; Lawrence et al., 2014). In AML, *MLL3* is contained within large hemizygous deletions that encompass all or part of the long arm of chromosome 7 and are common in treatment-associated myeloid neoplasms and complex karyotype AML but there is no evidence for homozygous inactivation of *MLL3* in leukemia (Jerez et al., 2012). In our studies, leukemia development triggered by *Mll3* shRNAs selected for an approximate 50% reduction in Mll3 rather than complete loss and

similarly, leukemia initiated by *Mll3* CRISPR/Cas9 contained both wild-type and mutant alleles. Hence, we propose that *MLL3* functions as a haploinsufficient tumor suppressor. Although our study focused on leukemia, our data imply that the heterozygous mutations in *MLL3* frequently observed in many tumor types may also be driving genetic events.

The function of MLL3, a histone methyltransferase, likely involves control of gene expression, and our studies suggest it plays an important role in controlling the normal differentiation of HSPC. Consistent with differentiation block of Mll3-suppressed HSPC, *Mll4* null pre-adipocytes have differentiation defects into adipocytes and myocytes (Lee et al., 2013), suggesting that Mll3/Mll4-containing COMPASS-like complex may generally play significant roles in the differentiation of stem cells and progenitors during normal development and homeostasis. However, Mll3 suppression is not sufficient to drive leukemogenesis but instead cooperates with p53 loss to impair the differentiation of hematopoietic stem and progenitor cells, resulting in an MDS-like state. Beyond this differentiation block, Mll3 suppression biased the development of disease to the myeloid lineage. This result was particularly striking because p53 deficiency is strongly associated with the development of lymphoid disease in mice (Donehower et al., 1992; Jacks et al., 1994). Although the mechanistic basis for this phenomenon remains to be determined, it is possible that other MLL family members, such as MLL2 (Pasqualucci et al., 2011), play a more important role in influencing the self-renewal and/or differentiation of the lymphoid lineage.

The genes affected by Mll3 suppression in mice were highly similar to those differentially expressed in HSCs from −7/del(7q) patients, implying that Mll3 is a major driver of 7q loss in human MDS and AML, and further supporting the relevance of our model to the human disease. Nonetheless, the failure of Mll3 to sustain an MDS phenotype in mice and the large scope of 7q deletions in patients imply that other 7q genes may contribute to tumor suppression as well. In this regard, 7q contains *EZH2*, a tumor suppressor in T-ALL (Ntziachristos et al., 2012; Simon et al., 2012); *MLL5*, another MLL family member that influences differentiation and self-renewal (Heuser et al., 2009; Madan et al., 2009; Zhang et al., 2009); and *CUX1*, a homeodomain protein whose suppression promotes the reconstitution of human hematopoietic cells in immunodeficient mice (McNerney et al., 2013). More work is clearly needed to test whether these 7q genes also promote AML in vivo, and if so, whether they interact with Mll3 in an additive, synergistic, or redundant manner.

The mouse model described here provides a murine model to approximate the genetics and behavior of 7q– and complex karyotype AML and recapitulate the marked chemoresistance of these diseases. As such, the model may serve as a useful pre-clinical system to test new therapies against these notoriously aggressive forms of AML. Accordingly, we showed that the BET inhibitor JQ1 has potent antileukemic effects in Mll3-suppressed cells, due to increased apoptosis and terminal differentiation associated with Myc suppression. Although the poor pharmacologic properties of JQ1 preclude a full characterization of the in vivo efficacy of Brd4 inhibition, our studies raise hope that next-generation BET inhibitors will be more effective at treating these aggressive AMLs than conventional therapies. A further understanding of the complex interactions between Mll3 and other haploinsufficient tumor

suppressors on 7q or in other AML-associated deletions may point toward yet other more rational approaches for patients with leukemia harboring −7/del(7q) lesions.

## EXPERIMENTAL PROCEDURES

### Human AML Genomics

The study was approved by the institutional review boards of the University of Chicago and Cold Spring Harbor Laboratory. Representational oligonucleotide microarray analysis (ROMA)-comparative genomic hybridization (CGH) analysis was performed on 52 AML samples—42 samples obtained at diagnosis, 3 at relapse, and 7 paired samples of diagnosis and subsequent relapse. DNA was hybridized to custom-designed arrays (ROMA) that can identify copy number changes with a resolution of ~35Kb (Hicks et al., 2006; Lucito et al., 2003). The Cancer Genome Atlas (TCGA) Tumorscape data were obtained from http://www.broadinstitute.org/tcga/home. The TCGA AML data set was downloaded from the TCGA data portal (https://tcga-data.nci.nih.gov/tcga/; Cancer Genome Atlas Research Network, 2013). Data were analyzed as described previously (Xue et al., 2012). SNP and somatic mutation data of 200 AML samples from TCGA were analyzed for chromosome 7/7q deletions, *MLL3* mutations, *NF1/RAS* pathway mutation, and *TP53* deletions/mutations.

### Mice

All the mouse experiments were approved by Cold Spring Harbor Laboratory Animal Use and Care Committee and the Institutional Animal Care and Use Committee at Memorial-Sloan Kettering Cancer Center. Retrovirus-infected HSPC ($1 \times 10^6$) were transplanted into sublethally irradiated (6 Gy, Cs137) C57Bl/6 mice (National Cancer Institution) by tail vein injection. For AML transplant experiments, $1 \times 10^6$ AML cells were transplanted into sublethally irradiated C57Bl/6 recipients. Mice were monitored for leukemogenesis by complete blood cell (CBC) test and blood smear staining. In drug treatment experiments, mice were treated by intraperitoneal injection of saline (vehicle) or 100 mg/kg cytarabine (araC, Bedford Laboratories) for 5 days and 3 mg/kg doxorubicin (Doxo, Bedford Laboratories) for 3 days. Mice were sacrificed and analyzed upon the moribund or indicated time point. JQ1 was delivered by gavage at the dose of 50 mg/kg/day for 7 days.

### shRNA Construction

Ninety-seven base-pair oligonucleotides with gene specific hairpins were ordered from Integrated DNA Technologies. The sequences were sh*Renilla*, 5′-TGCTGTTGACAGTGAGCGCAGGAATTATAATGCTTATCTATAGTGAAGC CACAGATGTATAGATAAGCATTATAATTCCTATGCCTACTGCCTCGGA-3′; and sh*Nf1*, 5′-TGCTGTTGACAGTGAGCGCGCTGGCAGTTTCAAACGTAATT AGTGAAGCCACAGATGTAATTACGTTTGAAACTGCCAGCATGCCTACTGC CTCGGA-3′; sh*Mll3*-1, 5′-TGCTGTTGACAGTGAGCGCGGAGACAAATATG TAGAGTTATAGTGAAGCCACAGATGTATAACTCTACATATTTGTCTCCTTGC CTACTGCCTCGGA-3′; and sh*Mll3*-2, 5′-TGCTGTTGACAGTGAGCGCACCA GTGATCACTTTACTAAATAGTGAAGCCACAGATGTATTTAGTAAAGTGATCA

CTGGTTTGCCTACTGCCTCGGA-3′. LMS (MSCV-mir30-SV40-GFP)-GFP and LMS-mCherry shRNAs were cloned as reported (Dickins et al., 2005; Scuoppo et al., 2012).

### CRISPR Construction

CRISPRs were designed at http://crispr.mit.edu provided by the Zhang laboratory and then cloned into pX330 CRISPR/Cas9 vector (Addgene) following Zhang's protocol (http://www.genome-engineering.org/crispr/?page_id=23). The target sequence of *Mll3* is TGCCAACCAGCACGCTTTAG and the control CRISPR sequence is GGCAGAAGGAACACAGGCTC.

Other experimental procedures are available in the Supplemental Experimental Procedures.

## Supplementary Material

Refer to Web version on PubMed Central for supplementary material.

## Acknowledgments

We thank N. Zhu, B. Bosbach, C. He, M. Taylor, J. Simon, C. Huang, and D. Grace for technical support and M. Spector, C. He, and J. Kendell for array CGH analysis of human AML. We thank C. Rillahan, J. Morris, L. Dow, J. Bolden, C. Sherr, and S. Mayack for comments on the manuscript. C.C. is supported by a career development fellowship from the Leukemia & Lymphoma Society. T.K. was supported by a DFG postdoctoral fellowship (KI1605/1-1). This work was supported by a program project grant from the NCI (to M.L.B. and K.S.) and a Specialized Center of Research (SCOR) grant from the LLS, a Starr Cancer Consortium grant (to C.V. and S.W.L.) and the Don Monti Memorial Research Foundation. S.W.L. is the Goeffrey Beene Chair of Cancer Biology at MSKCC and an Investigator in the Howard Hughes Medical Institute.

## References

Asou H, Matsui H, Ozaki Y, Nagamachi A, Nakamura M, Aki D, Inaba T. Identification of a common microdeletion cluster in 7q21.3 subband among patients with myeloid leukemia and myelodysplastic syndrome. Biochem Biophys Res Commun. 2009; 383:245–251. [PubMed: 19358830]

Balgobind BV, Van Vlierberghe P, van den Ouweland AM, Beverloo HB, Terlouw-Kromosoeto JN, van Wering ER, Reinhardt D, Horstmann M, Kaspers GJ, Pieters R, et al. Leukemia-associated NF1 inactivation in patients with pediatric T-ALL and AML lacking evidence for neurofibromatosis. Blood. 2008; 111:4322–4328. [PubMed: 18172006]

Bollag G, Clapp DW, Shih S, Adler F, Zhang YY, Thompson P, Lange BJ, Freedman MH, McCormick F, Jacks T, Shannon K. Loss of NF1 results in activation of the Ras signaling pathway and leads to aberrant growth in haematopoietic cells. Nat Genet. 1996; 12:144–148. [PubMed: 8563751]

Cancer Genome Atlas Research Network. Genomic and epigenomic landscapes of adult de novo acute myeloid leukemia. N Engl J Med. 2013; 368:2059–2074. [PubMed: 23634996]

Cong L, Ran FA, Cox D, Lin S, Barretto R, Habib N, Hsu PD, Wu X, Jiang W, Marraffini LA, Zhang F. Multiplex genome engineering using CRISPR/Cas systems. Science. 2013; 339:819–823. [PubMed: 23287718]

Corey SJ, Minden MD, Barber DL, Kantarjian H, Wang JC, Schimmer AD. Myelodysplastic syndromes: the complexity of stem-cell diseases. Nat Rev Cancer. 2007; 7:118–129. [PubMed: 17251918]

Dawson MA, Prinjha RK, Dittmann A, Giotopoulos G, Bantscheff M, Chan WI, Robson SC, Chung CW, Hopf C, Savitski MM, et al. Inhibition of BET recruitment to chromatin as an effective treatment for MLL-fusion leukaemia. Nature. 2011; 478:529–533. [PubMed: 21964340]

Dickins RA, Hemann MT, Zilfou JT, Simpson DR, Ibarra I, Hannon GJ, Lowe SW. Probing tumor phenotypes using stable and regulated synthetic microRNA precursors. Nat Genet. 2005; 37:1289–1295. [PubMed: 16200064]

Döhner H, Estey EH, Amadori S, Appelbaum FR, Büchner T, Burnett AK, Dombret H, Fenaux P, Grimwade D, Larson RA, et al. European LeukemiaNet. Diagnosis and management of acute myeloid leukemia in adults: recommendations from an international expert panel, on behalf of the European LeukemiaNet. Blood. 2010; 115:453–474. [PubMed: 19880497]

Donehower LA, Harvey M, Slagle BL, McArthur MJ, Montgomery CA Jr, Butel JS, Bradley A. Mice deficient for p53 are developmentally normal but susceptible to spontaneous tumours. Nature. 1992; 356:215–221. [PubMed: 1552940]

Grimwade D, Hills RK, Moorman AV, Walker H, Chatters S, Goldstone AH, Wheatley K, Harrison CJ, Burnett AK. National Cancer Research Institute Adult Leukaemia Working Group. Refinement of cytogenetic classification in acute myeloid leukemia: determination of prognostic significance of rare recurring chromosomal abnormalities among 5876 younger adult patients treated in the United Kingdom Medical Research Council trials. Blood. 2010; 116:354–365. [PubMed: 20385793]

Gui Y, Guo G, Huang Y, Hu X, Tang A, Gao S, Wu R, Chen C, Li X, Zhou L, et al. Frequent mutations of chromatin remodeling genes in transitional cell carcinoma of the bladder. Nat Genet. 2011; 43:875–878. [PubMed: 21822268]

Haferlach T. Molecular genetic pathways as therapeutic targets in acute myeloid leukemia. Hematology Am Soc Hematol Educ Program. 2008:400–411. [PubMed: 19074117]

Herz HM, Mohan M, Garruss AS, Liang K, Takahashi YH, Mickey K, Voets O, Verrijzer CP, Shilatifard A. Enhancer-associated H3K4 monomethylation by trithorax-related, the Drosophila homolog of mammalian Mll3/Mll4. Genes Dev. 2012; 26:2604–2620. [PubMed: 23166019]

Heuser M, Yap DB, Leung M, de Algara TR, Tafech A, McKinney S, Dixon J, Thresher R, Colledge B, Carlton M, et al. Loss of MLL5 results in pleiotropic hematopoietic defects, reduced neutrophil immune function, and extreme sensitivity to DNA demethylation. Blood. 2009; 113:1432–1443. [PubMed: 18854576]

Hicks J, Krasnitz A, Lakshmi B, Navin NE, Riggs M, Leibu E, Esposito D, Alexander J, Troge J, Grubor V, et al. Novel patterns of genome rearrangement and their association with survival in breast cancer. Genome Res. 2006; 16:1465–1479. [PubMed: 17142309]

Itzhar N, Dessen P, Toujani S, Auger N, Preudhomme C, Richon C, Lazar V, Saada V, Bennaceur A, Bourhis JH, et al. Chromosomal minimal critical regions in therapy-related leukemia appear different from those of de novo leukemia by high-resolution aCGH. PLoS ONE. 2011; 6:e16623. [PubMed: 21339820]

Ivanova NB, Dimos JT, Schaniel C, Hackney JA, Moore KA, Lemischka IR. A stem cell molecular signature. Science. 2002; 298:601–604. [PubMed: 12228721]

Jacks T, Remington L, Williams BO, Schmitt EM, Halachmi S, Bronson RT, Weinberg RA. Tumor spectrum analysis in p53-mutant mice. Curr Biol. 1994; 4:1–7. [PubMed: 7922305]

Jerez A, Sugimoto Y, Makishima H, Verma A, Jankowska AM, Przychodzen B, Visconte V, Tiu RV, O'Keefe CL, Mohamedali AM, et al. Loss of heterozygosity in 7q myeloid disorders: clinical associations and genomic pathogenesis. Blood. 2012; 119:6109–6117. [PubMed: 22553315]

Jones S, Chen WD, Parmigiani G, Diehl F, Beerenwinkel N, Antal T, Traulsen A, Nowak MA, Siegel C, Velculescu VE, et al. Comparative lesion sequencing provides insights into tumor evolution. Proc Natl Acad Sci USA. 2008; 105:4283–4288. [PubMed: 18337506]

Joslin JM, Fernald AA, Tennant TR, Davis EM, Kogan SC, Anastasi J, Crispino JD, Le Beau MM. Haploinsufficiency of EGR1, a candidate gene in the del(5q), leads to the development of myeloid disorders. Blood. 2007; 110:719–726. [PubMed: 17420284]

Kandoth C, McLellan MD, Vandin F, Ye K, Niu B, Lu C, Xie M, Zhang Q, McMichael JF, Wyczalkowski MA, et al. Mutational landscape and significance across 12 major cancer types. Nature. 2013; 502:333–339. [PubMed: 24132290]

Kelly LM, Gilliland DG. Genetics of myeloid leukemias. Annu Rev Genomics Hum Genet. 2002; 3:179–198. [PubMed: 12194988]

Kogan SC, Ward JM, Anver MR, Berman JJ, Brayton C, Cardiff RD, Carter JS, de Coronado S, Downing JR, Fredrickson TN, et al. Hematopathology Subcommittee of the Mouse Models of Human Cancers Consortium. Bethesda proposals for classification of nonlymphoid hematopoietic neoplasms in mice. Blood. 2002; 100:238–245. [PubMed: 12070033]

Lawrence MS, Stojanov P, Mermel CH, Robinson JT, Garraway LA, Golub TR, Meyerson M, Gabriel SB, Lander ES, Getz G. Discovery and saturation analysis of cancer genes across 21 tumour types. Nature. 2014; 505:495–501. [PubMed: 24390350]

Le DT, Kong N, Zhu Y, Lauchle JO, Aiyigari A, Braun BS, Wang E, Kogan SC, Le Beau MM, Parada L, Shannon KM. Somatic inactivation of Nf1 in hematopoietic cells results in a progressive myeloproliferative disorder. Blood. 2004; 103:4243–4250. [PubMed: 14982883]

Le Beau MM, Espinosa R 3rd, Davis EM, Eisenbart JD, Larson RA, Green ED. Cytogenetic and molecular delineation of a region of chromosome 7 commonly deleted in malignant myeloid diseases. Blood. 1996; 88:1930–1935. [PubMed: 8822909]

Lee MG, Villa R, Trojer P, Norman J, Yan KP, Reinberg D, Di Croce L, Shiekhattar R. Demethylation of H3K27 regulates polycomb recruitment and H2A ubiquitination. Science. 2007; 318:447–450. [PubMed: 17761849]

Lee CW, Arai M, Martinez-Yamout MA, Dyson HJ, Wright PE. Mapping the interactions of the p53 transactivation domain with the KIX domain of CBP. Biochemistry. 2009; 48:2115–2124. [PubMed: 19220000]

Lee JE, Wang C, Xu S, Cho YW, Wang L, Feng X, Baldridge A, Sartorelli V, Zhuang L, Peng W, Ge K. H3K4 mono- and di-methyltransferase MLL4 is required for enhancer activation during cell differentiation. eLife. 2013; 2:e01503. [PubMed: 24368734]

Liu TX, Becker MW, Jelinek J, Wu WS, Deng M, Mikhalkevich N, Hsu K, Bloomfield CD, Stone RM, DeAngelo DJ, et al. Chromosome 5q deletion and epigenetic suppression of the gene encoding alpha-catenin (CTNNA1) in myeloid cell transformation. Nat Med. 2007; 13:78–83. [PubMed: 17159988]

Lucito R, Healy J, Alexander J, Reiner A, Esposito D, Chi M, Rodgers L, Brady A, Sebat J, Troge J, et al. Representational oligonucleotide microarray analysis: a high-resolution method to detect genome copy number variation. Genome Res. 2003; 13:2291–2305. [PubMed: 12975311]

Madan V, Madan B, Brykczynska U, Zilbermann F, Hogeveen K, Döhner K, Döhner H, Weber O, Blum C, Rodewald HR, et al. Impaired function of primitive hematopoietic cells in mice lacking the Mixed-Lineage-Leukemia homolog MLL5. Blood. 2009; 113:1444–1454. [PubMed: 18952892]

Mali P, Yang L, Esvelt KM, Aach J, Guell M, DiCarlo JE, Norville JE, Church GM. RNA-guided human genome engineering via Cas9. Science. 2013; 339:823–826. [PubMed: 23287722]

Mann KM, Ward JM, Yew CC, Kovochich A, Dawson DW, Black MA, Brett BT, Sheetz TE, Dupuy AJ, Chang DK, et al. Australian Pancreatic Cancer Genome Initiative. Sleeping Beauty mutagenesis reveals cooperating mutations and pathways in pancreatic adenocarcinoma. Proc Natl Acad Sci USA. 2012; 109:5934–5941. [PubMed: 22421440]

March HN, Rust AG, Wright NA, ten Hoeve J, de Ridder J, Eldridge M, van der Weyden L, Berns A, Gadiot J, Uren A, et al. Insertional mutagenesis identifies multiple networks of cooperating genes driving intestinal tumorigenesis. Nat Genet. 2011; 43:1202–1209. [PubMed: 22057237]

McNerney ME, Brown CD, Wang X, Bartom ET, Karmakar S, Bandlamudi C, Yu S, Ko J, Sandall BP, Stricker T, et al. CUX1 is a haploinsufficient tumor suppressor gene on chromosome 7 frequently inactivated in acute myeloid leukemia. Blood. 2013; 121:975–983. [PubMed: 23212519]

Mrózek K. Cytogenetic, molecular genetic, and clinical characteristics of acute myeloid leukemia with a complex karyotype. Semin Oncol. 2008; 35:365–377. [PubMed: 18692687]

Ntziachristos P, Tsirigos A, Van Vlierberghe P, Nedjic J, Trimarchi T, Flaherty MS, Ferres-Marco D, da Ros V, Tang Z, Siegle J, et al. Genetic inactivation of the polycomb repressive complex 2 in T cell acute lymphoblastic leukemia. Nat Med. 2012; 18:298–301. [PubMed: 22237151]

Ong CK, Subimerb C, Pairojkul C, Wongkham S, Cutcutache I, Yu W, McPherson JR, Allen GE, Ng CC, Wong BH, et al. Exome sequencing of liver fluke-associated cholangiocarcinoma. Nat Genet. 2012; 44:690–693. [PubMed: 22561520]

Parsons DW, Li M, Zhang X, Jones S, Leary RJ, Lin JC, Boca SM, Carter H, Samayoa J, Bettegowda C, et al. The genetic landscape of the childhood cancer medulloblastoma. Science. 2011; 331:435–439. [PubMed: 21163964]

Pasqualucci L, Trifonov V, Fabbri G, Ma J, Rossi D, Chiarenza A, Wells VA, Grunn A, Messina M, Elliot O, et al. Analysis of the coding genome of diffuse large B-cell lymphoma. Nat Genet. 2011; 43:830–837. [PubMed: 21804550]

Patel JP, Gönen M, Figueroa ME, Fernandez H, Sun Z, Racevskis J, Van Vlierberghe P, Dolgalev I, Thomas S, Aminova O, et al. Prognostic relevance of integrated genetic profiling in acute myeloid leukemia. N Engl J Med. 2012; 366:1079–1089. [PubMed: 22417203]

Pellagatti A, Cazzola M, Giagounidis A, Perry J, Malcovati L, Della Porta MG, Jädersten M, Killick S, Verma A, Norbury CJ, et al. Deregulated gene expression pathways in myelodysplastic syndrome hematopoietic stem cells. Leukemia. 2010; 24:756–764. [PubMed: 20220779]

Qian Z, Joslin JM, Tennant TR, Reshmi SC, Young DJ, Stoddart A, Larson RA, Le Beau MM. Cytogenetic and genetic pathways in therapy-related acute myeloid leukemia. Chem Biol Interact. 2010; 184:50–57. [PubMed: 19958752]

Rücker FG, Bullinger L, Schwaenen C, Lipka DB, Wessendorf S, Frohling S, Bentz M, Miller S, Scholl C, Schlenk RF, et al. Disclosure of candidate genes in acute myeloid leukemia with complex karyotypes using microarray-based molecular characterization. J Clin Oncol. 2006; 24:3887–3894. [PubMed: 16864856]

Rücker FG, Schlenk RF, Bullinger L, Kayser S, Teleanu V, Kett H, Habdank M, Kugler CM, Holzmann K, Gaidzik VI, et al. TP53 alterations in acute myeloid leukemia with complex karyotype correlate with specific copy number alterations, monosomal karyotype, and dismal outcome. Blood. 2012; 119:2114–2121. [PubMed: 22186996]

Scuoppo C, Miething C, Lindqvist L, Reyes J, Ruse C, Appelmann I, Yoon S, Krasnitz A, Teruya-Feldstein J, Pappin D, et al. A tumour suppressor network relying on the polyamine-hypusine axis. Nature. 2012; 487:244–248. [PubMed: 22722845]

Shilatifard A. The COMPASS family of histone H3K4 methylases: mechanisms of regulation in development and disease pathogenesis. Annu Rev Biochem. 2012; 81:65–95. [PubMed: 22663077]

Silva JM, Li MZ, Chang K, Ge W, Golding MC, Rickles RJ, Siolas D, Hu G, Paddison PJ, Schlabach MR, et al. Second-generation shRNA libraries covering the mouse and human genomes. Nat Genet. 2005; 37:1281–1288. [PubMed: 16200065]

Simon C, Chagraoui J, Krosl J, Gendron P, Wilhelm B, Lemieux S, Boucher G, Chagnon P, Drouin S, Lambert R, et al. A key role for EZH2 and associated genes in mouse and human adult T-cell acute leukemia. Genes Dev. 2012; 26:651–656. [PubMed: 22431509]

Somervaille TC, Matheny CJ, Spencer GJ, Iwasaki M, Rinn JL, Witten DM, Chang HY, Shurtleff SA, Downing JR, Cleary ML. Hierarchical maintenance of MLL myeloid leukemia stem cells employs a transcriptional program shared with embryonic rather than adult stem cells. Cell Stem Cell. 2009; 4:129–140. [PubMed: 19200802]

Subramanian A, Tamayo P, Mootha VK, Mukherjee S, Ebert BL, Gillette MA, Paulovich A, Pomeroy SL, Golub TR, Lander ES, Mesirov JP. Gene set enrichment analysis: a knowledge-based approach for interpreting genome-wide expression profiles. Proc Natl Acad Sci USA. 2005; 102:15545–15550. [PubMed: 16199517]

Tie F, Banerjee R, Conrad PA, Scacheri PC, Harte PJ. Histone demethylase UTX and chromatin remodeler BRM bind directly to CBP and modulate acetylation of histone H3 lysine 27. Mol Cell Biol. 2012; 32:2323–2334. [PubMed: 22493065]

Xue W, Kitzing T, Roessler S, Zuber J, Krasnitz A, Schultz N, Revill K, Weissmueller S, Rappaport AR, Simon J, et al. A cluster of cooperating tumor-suppressor gene candidates in chromosomal deletions. Proc Natl Acad Sci USA. 2012; 109:8212–8217. [PubMed: 22566646]

Zang ZJ, Cutcutache I, Poon SL, Zhang SL, McPherson JR, Tao J, Rajasegaran V, Heng HL, Deng N, Gan A, et al. Exome sequencing of gastric adenocarcinoma identifies recurrent somatic mutations in cell adhesion and chromatin remodeling genes. Nat Genet. 2012; 44:570–574. [PubMed: 22484628]

Zhang Y, Wong J, Klinger M, Tran MT, Shannon KM, Killeen N. MLL5 contributes to hematopoietic stem cell fitness and homeostasis. Blood. 2009; 113:1455–1463. [PubMed: 18818388]

Zhao Z, Zuber J, Diaz-Flores E, Lintault L, Kogan SC, Shannon K, Lowe SW. p53 loss promotes acute myeloid leukemia by enabling aberrant self-renewal. Genes Dev. 2010; 24:1389–1402. [PubMed: 20595231]

Zuber J, Radtke I, Pardee TS, Zhao Z, Rappaport AR, Luo W, McCurrach ME, Yang MM, Dolan ME, Kogan SC, et al. Mouse models of human AML accurately predict chemotherapy response. Genes Dev. 2009; 23:877–889. [PubMed: 19339691]

Zuber J, Shi J, Wang E, Rappaport AR, Herrmann H, Sison EA, Magoon D, Qi J, Blatt K, Wunderlich M, et al. RNAi screen identifies Brd4 as a therapeutic target in acute myeloid leukaemia. Nature. 2011; 478:524–528. [PubMed: 21814200]

## Significance

Large deletions on 7q occur in a subset of AML that displays a particularly dismal prognosis, yet no AML tumor suppressors have been functionally validated in this region. We identify MLL3 as a 7q haploinsufficient tumor suppressor whose attenuation impairs the differentiation of HSPC and cooperates with other established AML lesions to drive leukemia in mice. Although murine and human AMLs with attenuated MLL3 function are resistant to conventional chemotherapy, they are sensitive to the BET inhibitor JQ1, suggesting a therapy for patients with these aggressive cancers. Additionally, our data imply that the frequent but poorly understood somatic mutations in *MLL3* occurring in many cancer types may actively contribute to tumorigenesis.

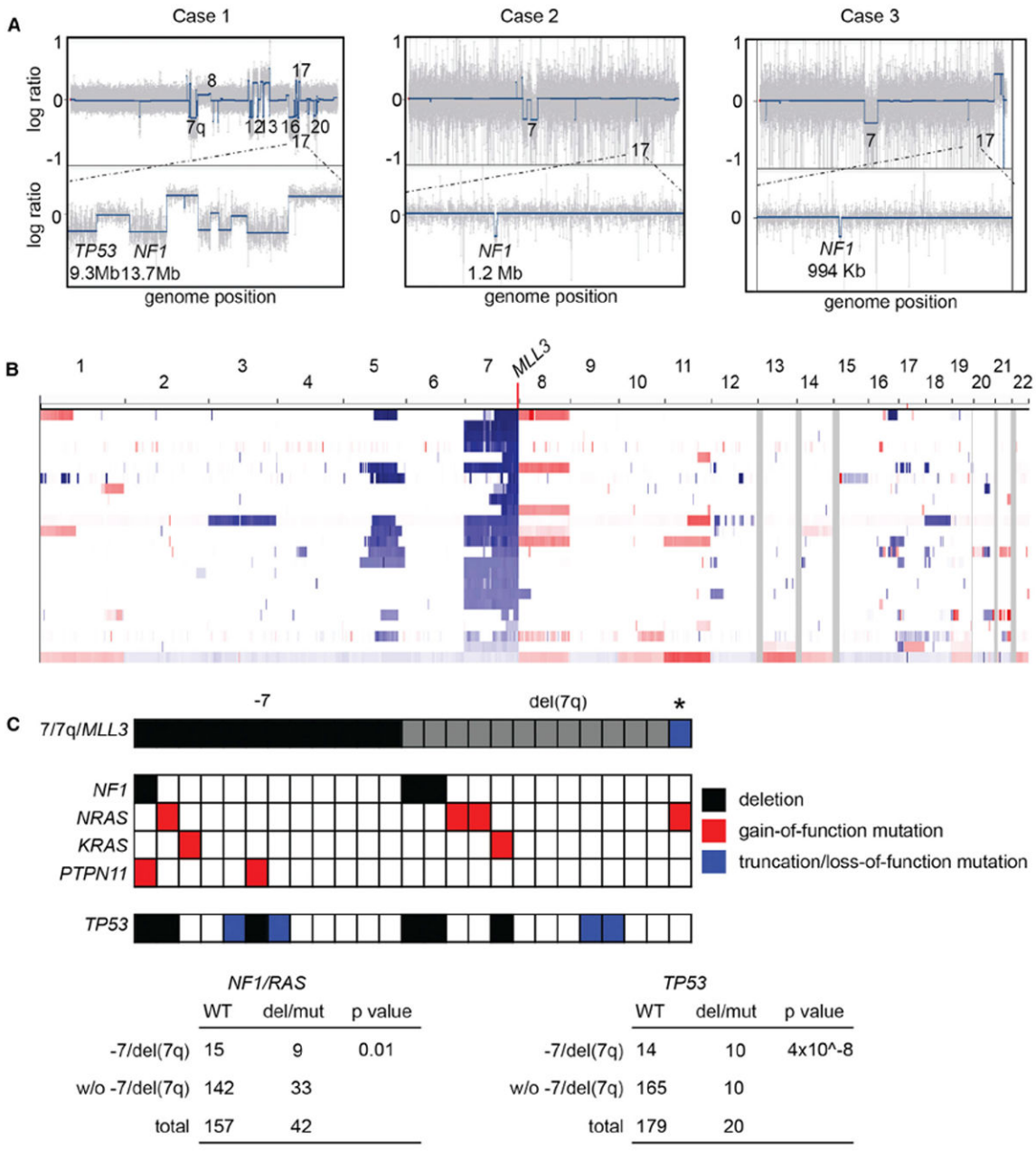


*NF1/RAS*

| | WT | del/mut | p value |
|---|---|---|---|
| -7/del(7q) | 15 | 9 | 0.01 |
| w/o -7/del(7q) | 142 | 33 | |
| total | 157 | 42 | |

*TP53*

| | WT | del/mut | p value |
|---|---|---|---|
| -7/del(7q) | 14 | 10 | 4x10^-8 |
| w/o -7/del(7q) | 165 | 10 | |
| total | 179 | 20 | |

**Figure 1. Chromosome 7 Loss or Deletion Is Associated with Mutations in *NF1/RAS* and *TP53* Pathways**

(A) ROMA plots depicting copy number changes of three AML cases. Data plotted are the normalized fluorescence log ratio for each probe (85 K). Top plot, whole genome view; left to right, chromosomes 1–22, X, Y. Bottom plots: high resolution of chromosome 17.

(B) Copy number events of the AML samples with chromosome 7 or 7q deletions (−7/del(7q)) in TCGA AML cohort. Blue, deletion; red, amplification.

(C) Top, heatmap of mutations in *NF1/RAS* pathways and *TP53* in −7/del(7q) and *MLL3* truncated (*) AML in the TCGA cohort. Black, deletions; red, gain-of-function mutations; blue, truncation or loss-of-function mutations. Bottom, the ratio of *NF1/RAS* and *TP53*

mutations in −7/del(7q) compared to AML samples without −7/del(7q). p value was calculated by chi-square test.

See also Figure S1.

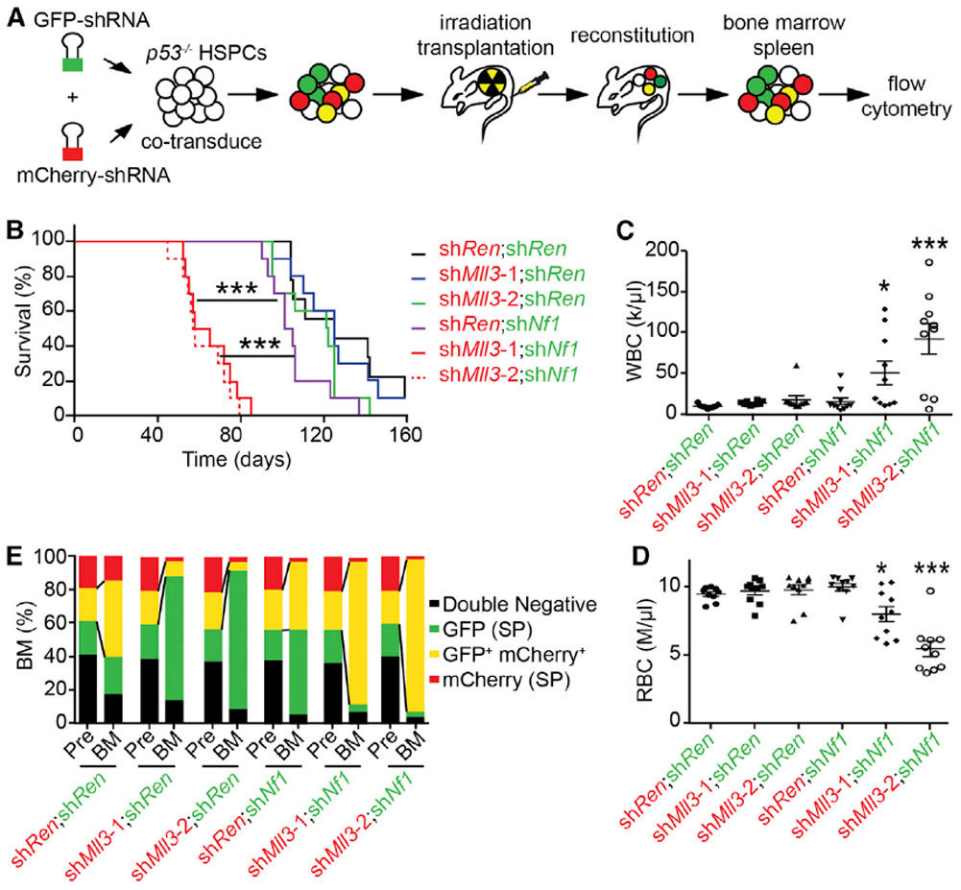


**Figure 2. RNAi-Mediated Cosuppression of Mll3 and Nf1 Cooperates with p53 Loss to Promote Myeloid Leukemogenesis**

(A) Schematic experimental design. *p53*$^{-/-}$ HSPC were co-infected with GFP-linked and mCherry-linked shRNAs and then transplanted into sublethally irradiated recipient mice.

(B–D) The recipient mice were then monitored for disease in a variety of ways including overall survival (B) as well as WBC (C) and red blood cell (D) counts (n = 10, 8 weeks posttransplant or upon death of leukemia-bearing sh*Mll3*;sh*Nf1;p53*$^{-/-}$ recipients if they died before 8 weeks), showing mean ± SD.

(E) After sacrifice, the BM was harvested and analyzed by flow cytometry to determine the frequency double negative, GFP$^{+}$, mCherry$^{+}$, and double positive cells, as compared to their frequency pre-injection (Pre).

In all experiments, n = 10 except in (E) where n = 3–4. *p < 0.05; **p < 0.01; ***p < 0.001. See also Figure S2.

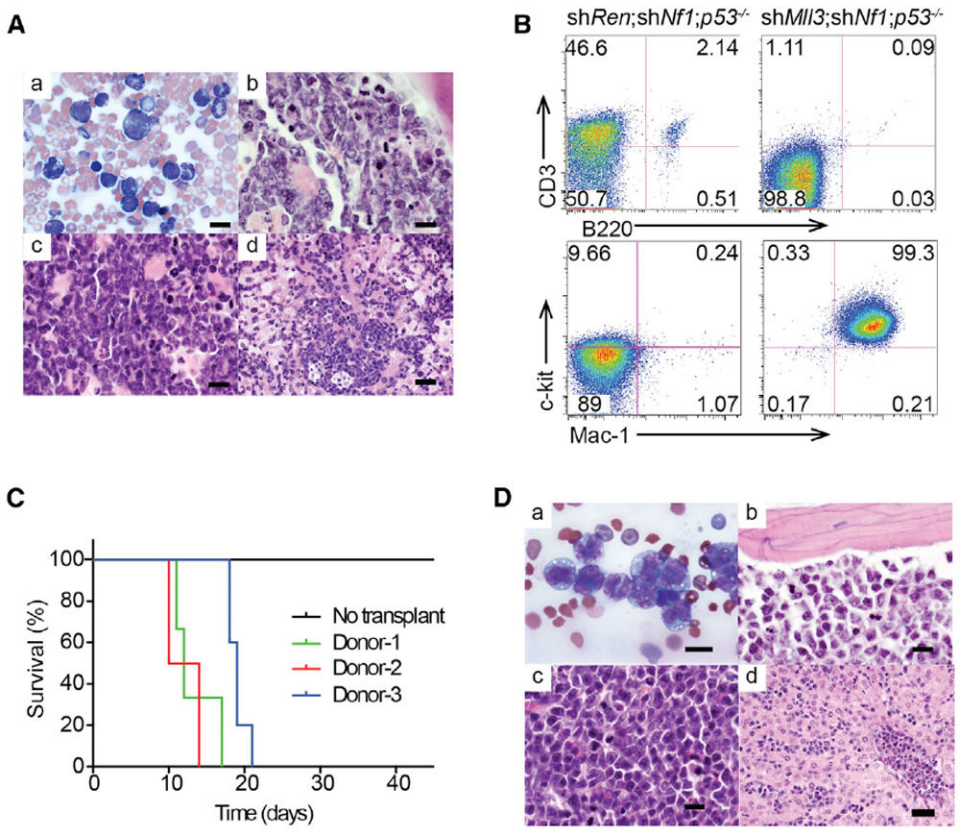


**Figure 3. Characterization of MNP AML**

(A) Histological analysis of blood (a), liver (b), spleen (c), and BM (d) of an MNP recipient mouse. Scale bar: 12 μm for (a–c) and 30 μm for (d).

(B) Representative flow cytometry profiles of GFP/mCherry double-positive cells from BM of MNP recipient mice versus control mice (sh*Ren*;sh*Nf1;p53*$^{-/-}$ are shown; all other control groups are similar, not shown). Left: lymphocyte markers B220 and CD3; right: myeloid marker Mac-1 and stem cell marker c-kit.

(C) Survival of secondary transplant recipient mice of three independent MNP AML. n = 5 per group.

(D) Histological analysis of secondary transplant recipient mice of MNP AML. (a) blood smears, (b) section of bone marrow, (c) section of spleen, and (d) section of liver. Scale bar: 12 μm for (a–c) and 30 μm for (d).

See also Figure S3.

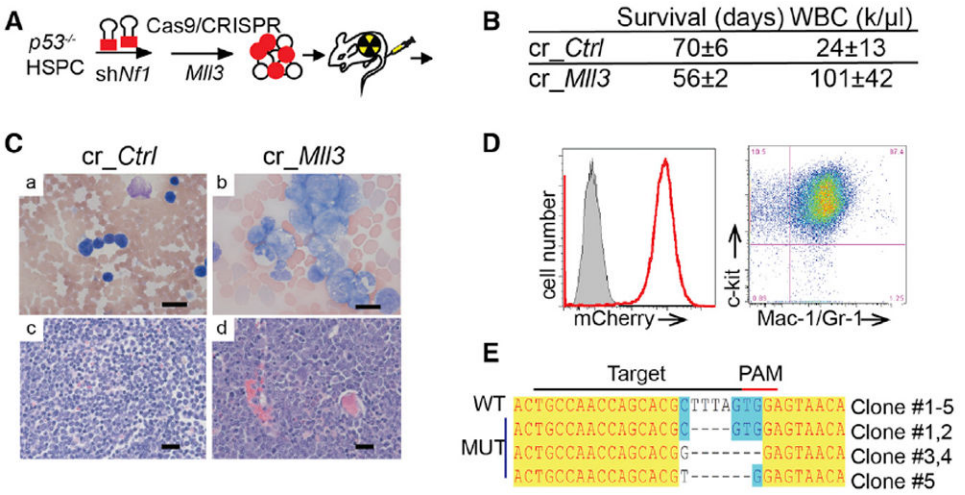


**Figure 4. In Vivo CRISPR/Cas9 Confirmed that Mll3 Is a Haploinsufficient Tumor Suppressor in AML**

(A) Schematic experimental design. *p53*$^{-/-}$ HSPC were transduced with mCherry-sh*Nf1* and then CRISPR/Cas9 constructs targeting a control, noncoding region on chromosome 8 (cr_Ctrl) or *Mll3* (cr_*Mll3*) were transiently introduced by electroporation, and transplanted into sublethally irradiated recipient mice.

(B) The average survival and WBC counts of recipient mice transplanted with cr_Ctrl;sh*Nf1;p53*$^{-/-}$ and cr_*Mll3*;sh*Nf1;p53*$^{-/-}$ HSPC, showing mean ± SD (n = 3).

(C) Blood smear and BM sections of recipient mice transplanted with cr_Ctrl;sh*Nf1;p53*$^{-/-}$ and cr_*Mll3*;sh*Nf1;p53*$^{-/-}$ HSPC. Scale bar: 12 μm.

(D) Flow cytometry analysis of cr_*Mll3*;sh*Nf1;p53*$^{-/-}$ AMLs shows the expressions of mCherry and myeloid surface markers c-kit and Mac-1/Gr-1.

(E) The sequences of the wild-type *Mll3* region targeted by CRISPR/Cas9, and the resulting insertions/deletions detected in various cr_*Mll3* leukemia clones.

See also Figure S4.

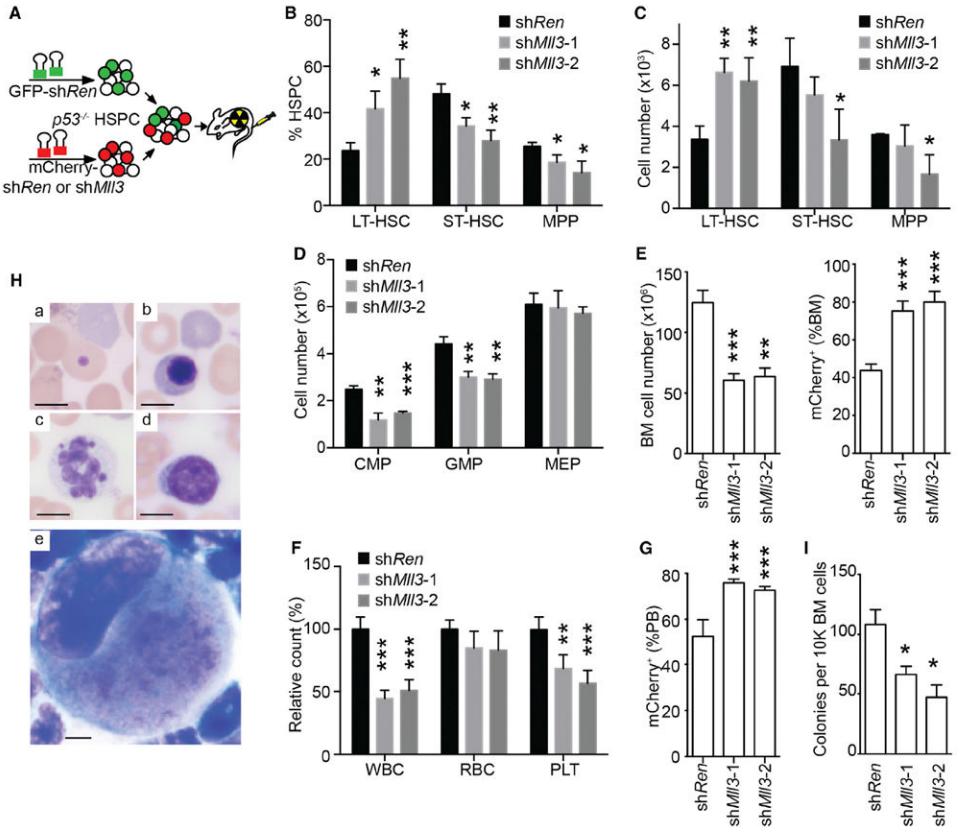


**Figure 5. Mll3 Inhibition Blocks HSPC Differentiation and Results in an MDS-like Syndrome in Mice**

(A) Schematic experimental design. *p53*$^{-/-}$ HSPC were transduced with GFP– *Ren* or mCherry-linked *Ren* or *Mll3* shRNAs. One day after infection, GFP+ and mCherry+ HSPC were mixed at a 1:1 ratio and transplanted into lethally irradiated syngeneic recipient mice.

(B) The percentage of LT-HSC (Flt3$^{-}$lin$^{-}$Sca-1$^{+}$c-kit$^{+}$CD150$^{+}$CD48$^{-}$CD34$^{-}$), ST-HSC (Flt3$^{-}$lin$^{-}$Sca-1$^{+}$c-kit$^{+}$CD150$^{+}$CD48$^{+}$CD34$^{-}$) and MPP (Flt3$^{-}$lin$^{-}$Sca-1$^{+}$ c-kit$^{+}$CD150$^{-}$CD48$^{+}$CD34$^{-}$) in the mCherry$^{+}$ HSC (Flt3$^{-}$lin$^{-}$Sca1$^{+}$c-kit$^{+}$CD34$^{-}$) population at 6 weeks after transplant. n = 3.

(C) The absolute numbers of LT-HSC, ST-HSC, and MPP in the BM of recipient mice at 6 weeks after transplant. n = 3.

(D) The absolute numbers of common myeloid progenitor (CMP; Flt3$^{-}$lin$^{-}$Sca1$^{-}$c-kit$^{+}$CD34$^{+}$CD16/32$^{-}$), granulocyte-macrophage progenitor (GMP; Flt3$^{-}$lin$^{-}$ Sca1$^{-}$c-kit$^{+}$CD34$^{+}$CD16/32$^{+}$) and megakaryocyte erythrocyte progenitor (MEP; Flt3$^{-}$lin$^{-}$Sca1$^{-}$c-kit$^{+}$CD34$^{-}$CD16/32$^{-}$) in the BM of recipient mice at 6 weeks after transplant. n = 3.

(E) Left, the BM cellularity of sh*Ren;p53*$^{-/-}$ and sh*Mll3;p53*$^{-/-}$ mice at 6 weeks after transplant. Right, reconstitution ratio of mCherry$^{+}$ donor cells in BM at 6 weeks after transplantation. n = 5.

(F) White blood cell (WBC), red blood cell (RBC), and platelet (PLT) counts in sh*Mll3* recipient mice compared to sh*Ren* control mice at 6 weeks after transplant. n = 5.

(G) Reconstitution ratio of mCherry+ donor cells in the peripheral blood at 6 weeks after transplantation. n = 5.

(H) Representative pictures showing dysplastic blood and BM cells from sh*Mll3;p53*$^{-/-}$ mice at 6 weeks after transplant. Howell Jolly body in peripheral blood (a); nucleated RBC in peripheral blood (b); hypersegmented neutrophil in peripheral blood (c); blast in peripheral blood (d); dysplastic megakaryocytes in BM (e). Scale bar: 5 μm.
(I) Number of colonies formed per 10,000 BM cells from sh*Ren;p53*$^{-/-}$ or sh*Mll3;p53*$^{-/-}$ recipient mice 6 weeks after transplant. n = 3. (B–G) and (I) show mean ± SD. *p < 0.05; **p < 0.01; ***p < 0.001.
See also Figure S5.

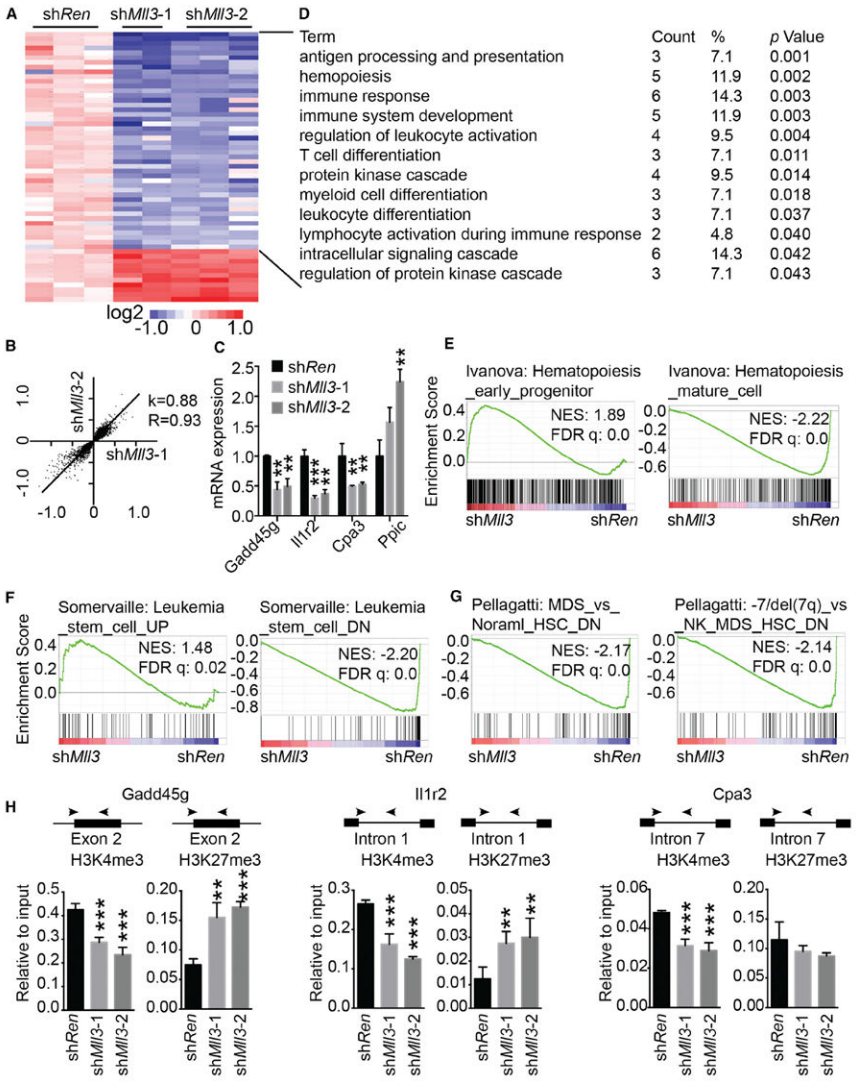


**Figure 6. Mll3 Suppression Enforces a Self-Renewal Gene Expression Program by Altering Chromatin Modifications**

(A) Differentially expressed genes in sh*Mll3;p53*$^{-/-}$ HSPC compared to sh*Ren;p53*$^{-/-}$ HSPC (>1.5-fold different expression values, $\log_2$; $p < 0.05$ by two-way Student's t test), as revealed by Illumina microarray gene expression analysis.

(B) The correlation of the gene signatures between sh*Mll3-1* and sh*Mll3-2*. The fold changes of the differently expressed genes ($p < 0.05$) in sh*Mll3-1;p53*$^{-/-}$ HSPC (versus sh*Ren;p53*$^{-/-}$ HSPC) and sh*Mll3-1;p53*$^{-/-}$ HSPC (versus sh*Ren;p53*$^{-/-}$ HSPC) were plotted as X and Y, respectively. $k = 0.88$ and Pearson's coefficient $R = 0.93$.

(C) qPCR confirmation of gene expression changes using cDNA of FACS purified LT-HSC ($Flt3^{-}lin^{-}Sca\text{-}1^{+}c\text{-}kit^{+}CD150^{+}CD48^{-}CD34^{-}$) from sh*Ren;p53*$^{-/-}$ or sh*Mll3;p53*$^{-/-}$ recipient mice 6 weeks after transplant. n = 3.

(D) Summary of the top functional categories of genes significantly enriched in sh*Mll3;p53*$^{-/-}$ HSPC. Analyses were performed on downregulated genes in sh*Mll3;p53*$^{-/-}$ HSPC, using DAVID (http://david.abcc.ncifcrf.gov/tools.jsp).

(E) GSEA of sh*Mll3;p53*$^{-/-}$ HSPC expressing profile using a hematopoietic early progenitor-associated signature (NES = 1.89; FDR q = 0.0) and a mature hematopoietic cell-associated signature (NES = –2.22; FDR q = 0.0).

(F) GSEA of sh*Mll3;p53*$^{-/-}$ HSPC expressing profile using a leukemic stem cell (LSC)-associated upregulated signature (NES = 1.48; FDR q = 0.02) and an LSC-associated downregulated signature (NES = −2.20; FDR q = 0.0).

(G) Left, GSEA of sh*Mll3;p53*$^{-/-}$ HSPC expressing profile using a downregulated gene signature in human MDS HSC (versus normal HSC; NES = −2.17, FDR q = 0.0); right, GSEA of sh*Mll3;p53*$^{-/-}$ HSPC expressing profile using a downregulated gene signature in human −7/del(7q) MDS HSC (versus normal karyotype MDS HSC; NES = –2.14, FDR q = 0.0).

(H) Upper, ChIP-qPCR showing the levels of H3K4me3 and K3K27me3 at loci of Gadd45 g, Il1r2 and Cpa3 in sh*Ren;p53*$^{-/-}$ and sh*Mll3;p53*$^{-/-}$ HSPC, with two biological repeats and two technical repeats for each sample. Lower, the locations of qPCR amplicons in target genes.

(C) and (H) show mean ± SD. **p < 0.01; ***p < 0.001. See also Table S1.

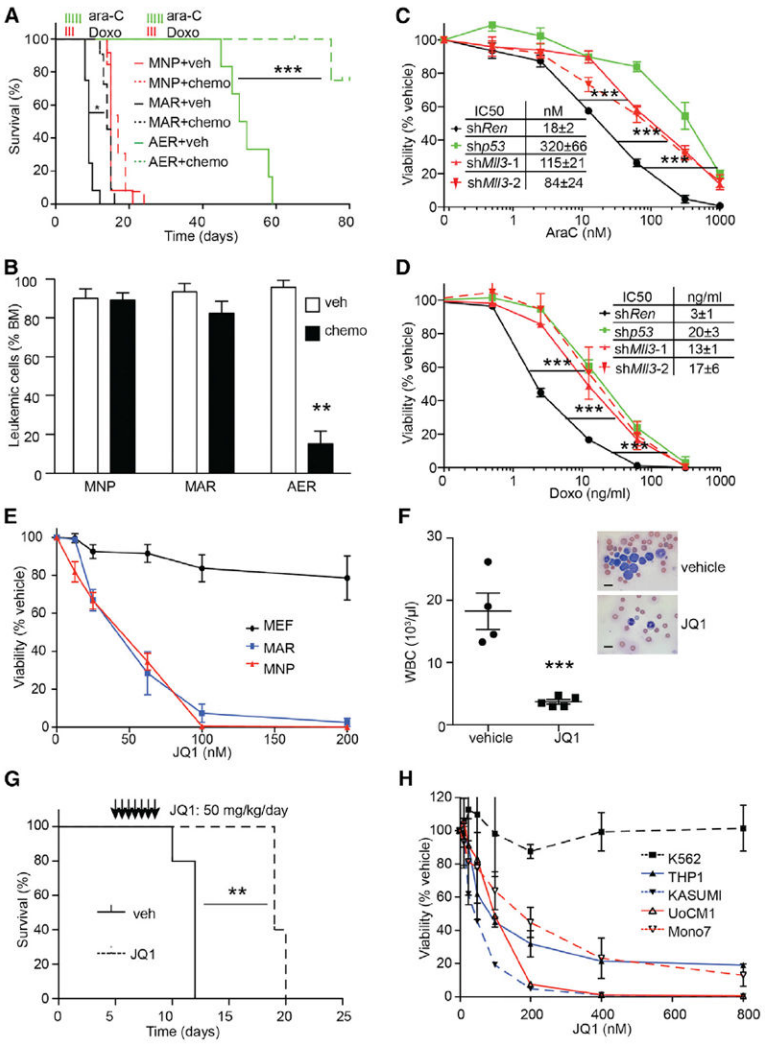


**Figure 7. Murine AMLs with Mll3 Suppression Are Resistant to Conventional Chemotherapy**

(A and B) In vivo treatment of mice transplanted with sh*Mll3*;sh*Nf1;p53*$^{-/-}$ (MNP), *MLL-AF9; Nras*$^{G12D}$ (MAR) or *AML1-ETO;Nras*$^{G12D}$ (AER) AML with chemotherapy. Recipient mice were transplanted with MNP (n = 12), MAR (n = 12), or AER (n = 6 for veh, 7 for chemo), leukemic cells (CD45.2$^{+}$) at day 0. Mice were treated with 100 mg/kg cytarabine (AraC) for 5 days and 3 mg/kg doxorubicin (Doxo) for 3 days by intraperitoneal injections starting at day 3 (MNP and MAR) or day 25 (AER) post-transplant. Kaplan-Meier survival curves of mice bearing MNP leukemias with or without chemotherapy treatment (A). Percentages of tumor cells in the bone marrow of terminal recipient mice, or at sacrifice 65 days after transplant in the case of the AER vehicle-treated group (B). n = 3. **p < 0.01, two-tail student t test.

(C and D) AER AML cells were transduced with sh*Ren*, sh*p53*, or sh*Mll3* and then treated with indicated concentrations of AraC (C) or Doxo (D) for 3 days. Cell number was normalized to vehicle-treated cells. Graphs represent the average of four independent experiments and insets display half-maximal inhibitory concentration values. ***p < 0.001, two-way ANOVA test.

(E) Dose response of MNP and MAR AML and MEFs to JQ1 in vitro. Cells were treated with vehicle or 1–200 nM JQ1 for 3 days and viable cells were counted by flow cytometry and cell numbers were normalized to vehicle-treated controls. Graph shows an average of three independent experiments.

(F and G) MNP recipient mice were treated with vehicle or 50 mg/kg/day JQ1 by gavage for 1 week starting at 5 days after transplant. (F) left, WBC counts of MNP mice treated with vehicle or JQ1, 12 days after transplantation (n = 5). Right, blood smear of mice at day 12 after transplantation. Scale bar: 10 μm. (G) Survival curve of recipient mice.

(H) Dose response of human AML cell lines to JQ1. Cells were treated with vehicle or 1–200 nM JQ1 for 3 days. Graphs represent the average of three independent experiments performed as described in (E).

(C–F) and (H) show mean ± SD. See also Figure S6.